Size and transparency influence diel vertical migration patterns in copepods.

Alex Barth ????? Joshua Stone

21 Mar 2023

1 Abstract

Diel vertical migration (DVM) is a widespread phenomenon in aquatic environments. The primary hypothesis explaining DVM is the visual predator evasion hypothesis, which suggests that zooplankton migrate to deeper waters to avoid detection during daylight. However, visual risk also depends on a copepod's morphology. In this study, we investigate hypotheses related to morphology and DVM: (H1) size increases visual risk and will increase DVM and (H2) copepod transparency will reduce visual risk and thus reduce DVM. Copepod images were collected across several cruises in the Sargasso Sea using an Underwater Vision Profiler 5. Copepod morphology was characterized from these images and a dimension reduction approach. The results show a clear relationship in which larger copepods have a larger DVM signal. Darker copepods appear to have a larger DVM signal, however only amongst the largest group of copepods. This suggest a complex relationship between copepod morphology and behavior.

2 *Scientific Significance Statement*

Diel Vertical Migration is a widespread phenomenon across marine and freshwater systems. The predator evasion hypothesis suggests that DVM occurs as zooplankton attempt to escape visual predators. Yet, DVM itself is a costly and risky behavior. Thus, DVM should only occur when visual risk is high. Several studies have shown that copepod size influences the magnitude of DVM. However, an individual's visual risk may include traits beyond simply size. In this study, we utilize an in-situ imaging tool to reveal how copepod morphological traits influence DVM. Our findings show that both size and transparency influence DVM. This finding highlights that DVM is a complex behavior driven by copepod traits. Furthermore, this study exemplifies the ability of new technology to draw insights into plankton ecology.

3 Introduction

Diel vertical migration (DVM) is a wide spread phenomena with large consequences in ocean ecosystems. DVM is the process of pelagic organisms vertically moving in the water column on a daily basis, often travelling dozens to hundreds of meters (Bianchi and Mislan 2016). This large-scale event occurs across many taxa, from plankton to fish (Brierley 2014). However, DVM is particularly notable in zooplankton communities, whose migrations contribute substantially to biogeochemical cycles (Steinberg and Landry 2017; Archibald et al. 2019; Siegel et al. 2023). Zooplankton communities, largely dominated by copepods (Turner 2004), will feed in surface layers of the ocean then migrate into deeper waters. Through this movement,

copepods actively transport carbon to depth. Additionally, Kelly et al. (2019) described zooplankton DVM to be a major component of mesopelagic food webs. Thus it is critically important to understand the drivers of DVM.

Predominantly, zooplankton DVM is the movement from deep waters at daytime to shallower waters at night (Hays 2003; Bianchi and Mislan 2016). The leading explanation for this pattern is the predator-avoidance hypothesis (Bandara et al. 2021). This hypothesis posits zooplankton evacuate the sunlit surface to evade visual predators then ascend at night to feed. However, the massive migration undertaken by these copepods is energetically expensive (Maas et al. 2018). Therefore, the visual predator evasion hypothesis implies that DVM is a result of visual risk exceeding migration costs. However, a copepod's visual risk to a visual predator depends morphological features (Aksnes and Utne 1997). Notably a copepod's size can increase visual detection. Several studies have documented that copepod size influences DVM magnitude (Hays et al. 1994; Aarflot et al. 2019). Presumably, a copepod's transparency will also influence DVM. Hays et al. (1994) reported that pigmentation explained variation in DVM frequency. However, few other studies have investigated this at length. One barrier to studying a relationship between copepod morphology and DVM is the difficulty of accurately recording traits.

In-situ imaging tools offer great potential to better describe copepod DVM. By directly observing a copepod, new insights into their behavior and traits can be resolved (Ohman 2019). For example, Whitmore and Ohman (2021) used an in-situ imaging device to describe a relationship of copepod abundance with a particulate field rather than chlorophyll-a. Such findings

are facilitated by the fact imagery data records an individual's exact position. Additionally, a copepod's true appearance can be documented whereas net-collected organisms are often deformed or lacking color. Some studies have noted a copepod DVM with in-situ imagery data (Pan et al. 2018; Whitmore and Ohman 2021). However, direct tests of DVM-related hypotheses with such data have not been conducted.

In this study, we utilized in-situ imaging to evaluate how copepod morphological traits influence patterns. We specifically test the hypotheses that, (H1) size increases visual risk and will increase DVM and (H2) copepod transparency will reduce visual risk and thus reduce DVM. If these morphologically based hypotheses are true, then the larger and darker copepods will have the largest DVM signals.

4 Methods

4.1 CTD profiles and UVP imaging of copepods

Data were collected aboard the R/V Atlantic Explorer in collaboration with the Bermuda Atlantic Time-series Study (BATS) (Steinberg et al. 2001). In-situ images of plankton were acquired using an Underwater Vision Profiler (UVP5) (Picheral et al. 2010). The original sampling methodology and instrument specification followed details described in (Barth and Stone 2022). The UVP was attached to the CTD rosette and deployed intermittently on cruises to the Sargasso Sea from June 2019 - December 2021. Typical monthly cruises included ~13 profiles with average descents to 1200m (Supplemental Figure 1). In this study, we investigated

general trends in DVM by pooling together casts across multiple cruises. This approach is necessitated by the small sampling volume of the UVP and low abundance of plankton which requires aggregation of data to resolve trends (Barth and Stone 2022). While there was some variation between cruises (Supplemental Figure 2), this oligotrophic system is relatively consistent across seasons. Additionally, every cruise had an approximately equal number of day and night casts. Profiles were assigned to be day or night based on locally calculated nautical dawn and nautical dusk times using the R package `suncalc 0.5.1`.

The UVP records images of large particles (>600μm ESD). However, living particles are not reliably identifiable below 0.9 mm (Barth and Stone 2022). All recorded images were processed using Zooprocess (Gorsky et al. 2010), which provides several metrics related to size, grey value, and shape complexity. These features were then used to automatically sort images using Ecotaxa (Picheral et al.). All images were manually verified by the same trained taxonomist. In total, 294,913 images were recorded. Of these, 85.2% were images of debris or artefacts. The smallest identified copepod was 0.940mm ESD and the largest was 5.904mm ESD. Across all casts, copepods were the most common organism, composing 58.7% of all identified, living particles. In total, there were 4151 individual copepods images.

4.2 Morphological Grouping

The UVP automatically measures and collects several morphologically relevant parameters. To create relevant groups of copepods, a dimension reduction and clustering approach was used. Similar methods have been successfully utilized to provide novel insights to marine snow

(Trudnowska et al. 2021), copepod dynamics in the Arctic (Vilgrain et al. 2021), and temporal trends in phytoplankton communities (Sonnet et al. 2022). First, 18 morphologically relevant parameters were selected to be included in a principal Components Analysis (PCA), following (Vilgrain et al. 2021). Parameters can be described as relating to size (e.g. major axis, feret diameter, ESD), grey intensity (e.g. mean grey value), shape (e.g. elongation, symmetry), and shape complexity (e.g. fractal dimension). The PCA was weighted by the volume sampled in a 1-m depth bin for each observation. This approach provides a correction for the UVP's variable descent speed which can cause duplicate imaging of individuals. While this phenomena has a minor impact on overall results (Barth and Stone 2022), we used the weighted approach to assure that no individual features were overrepresented. All morphological descriptors were scaled and centered prior to inclusion in the analysis. The model was constructed using the R package `FactoMineR 2.7`. principal components were deemed to be significant if their eigenvalues were greater than 1. This approach yielded 4 PCs which described 87.3% of the total variation in morphological parameters, with 34.5% and 26.5% in the first two components respectively. This four principal component space provides a "morphospace" to characterize copepods.

To address our morphology-DVM hypotheses, we constructed discrete morphological groups based on the first two principal components. Groups along each of the principal components were defined as low (below 25th percentile), mid (25th-75th percentile) and high (greater than 75th percentile). To address the size-dependent hypothesis (H1), groups were assigned as low, mid, or high along PC1. Then to assess if color/transparency was a secondary factor (H2),

within each PC1 group, PC2 groups were constructed as low, mid, or high. In total, this created 9 groups (e.g. Low PC1-Low PC2, Low P1-mid PC2, etc).

4.3 Copepod vertical structure & DVM

4.3.1 Vertical distribution of copepods

Copepods in this system are well documented to undergo DVM (Steinberg et al. 2000; Schnetzer and Steinberg 2002; Maas et al. 2018) However, there have not been direct measurements of DVM with in situ imaging data. First, to assess which portion of the water column copepods were utilizing for DVM, we visualized the average vertical structure. The concentration of each morphological group (based on PC1 and PC2) were calculated in 20m depth bins for each UVP profile. These binned-profiles were then averaged together based on time of day.

4.3.2 Weighted mean depth variability

Weighted mean depth (WMD) is a common metric to describe vertical structure and DVM in zooplankton (Ohman et al. 2002; Ohman and Romagnan 2016; Aarflot et al. 2019). However, with in-situ imagery, this approach presents a few challenges. WMD cannot be calculated individually for each profile then averaged because each profile had a different descent depth. Additionally, the small and uneven sampling volume of the UVP can make single casts inaccurate. Yet, understanding variation around the WMD is necessary to compare DVM strength across groups. Here, we introduce a depth-bin constrained bootstrap approach to define WMD

with a 95% confidence interval. To do this, the concentration of each group, was calculated in 20m depth bin for each profile. Then all profiles from the same time of day were 'pooled'. This provides a distribution of concentrations in each depth-bin. Traditional bootstrapping randomly samples, with replacement, all observations. With vertically structured data however, full random sampling would bias estimates towards the surface. To avoid this, samples were "bin-constrained" such that for each iteration, a random observation was sampled within each depth bin, then replaced for the next iteration. A maximum depth was set to 600m, as it is unlikely that typical copepod DVM extends beyond this point. This approach effectively created a random profile by resampling a concentration, $conc^*$, from each depth bin, d. This profile then was used to calculate a bootstrapped weighted mean depth, WMD^*. This was done for each morphological group g, at each time of day t.

$$WMD^*_{g,t} = \sum_{i}^{N=60} \frac{d_i(conc^*_{i,g,t})}{\sum_i^{N=60} conc^*_{i,g,t}}$$

The distribution of $WMD^*_{g,t}$ then was used to calculate a bootstrapped mean and 95% confidence interval. The 95% CIs could be compared between times of day and morphological groups to assess the strength of DVM. Using PC1 to assess size, the WMD was compared between the three PC1-groups by percentile level. Then to assess the effect of transparency the WMD was compared between PC2-groups within each PC1-grouping. A larger signal of DVM would be evident by a clearly deeper (non-overlapping 95% CI) daytime WMD.

4.4 Data availability

All data and code are made available via (https://github.com/TheAlexBarth/DVM_Migration-Morphology). All supplemental figures, tables, and analyses are hosted on a public static site (https://thealexbarth.github.io/DVM_Migration_Morphology).

5 Results

5.1 Morphological Groups

The PCA revealed four major axis of variability (Figure 1). The first axis (PC1, 34.23% of variability) was largely explained by increasing values related to size, such as perimeter (loading score = 0.927) and feret diameter (loading score = 0.910). The second axis (PC2, 27.24% of variability) can be interpreted as a gradient of transparent to dark individuals. PC2 was largely anticorrelated with mean grey value (higher values indicate a more transparent individual) (loading score = -0.920). As noted in the methods, PC3 and PC4 were both related to the orientation of the copepod and the appendage visibility respectively (Supplemental Figure 3).

The morphological groupings were assigned along PC1 as low, mid and high. Then along PC2, groups were assigned within each PC1-group (Figure 1). To confirm the morphospace grouping resulted in ecologically relevant categories, the morphological groups were compared against known copepod metrics. Across all PC1-groups, there was a clear difference in feret diameter.

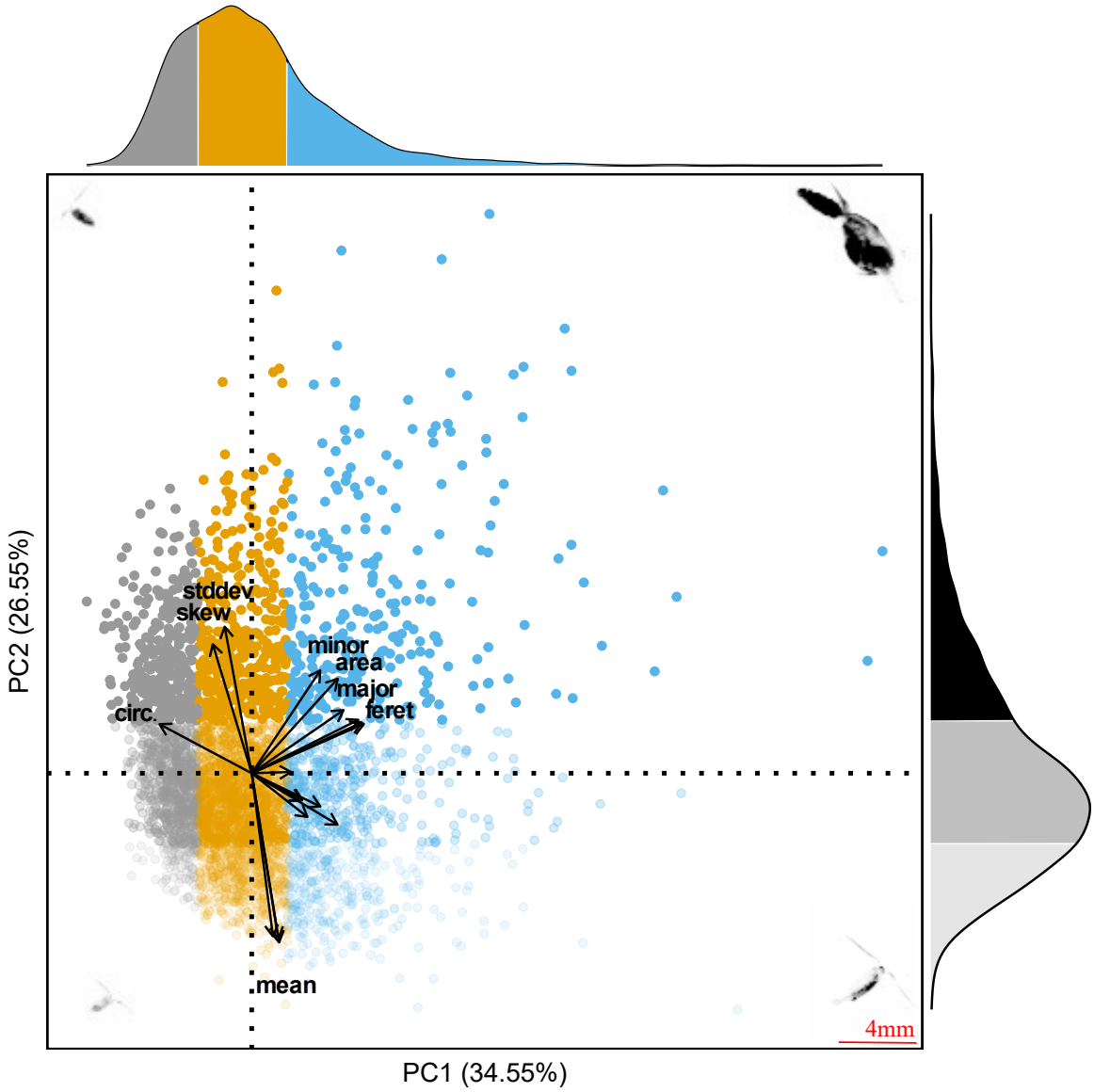

Figure 1: First two principal components of the morphospace. Proportion of variance explained by the two axis is . Each point represents an individual copepod. The color and transparency of each point corressponds to the morphological groups based on pecentile along each axis. Marginal distribution display the proportion of observations in each group. Representative vignettes of copepods are shown in the corners corresponding to their place in the morphospace. 4mm scale bar in the bottom right is shown for the vignettes.

The median feret diameter of the low group was 1.97mm. The median feret diameter of the mid and high groups were 2.84mm and 4.83mm, respectively (Figure 2A). All groups were significantly different from one another (Dunn Kruskall-Wallace test, $p < 0.001$). PC2 groups as a whole were also significantly different from one another (Dunn Krustall-wallace test, $p < 0.001$). However, within each PC2-group, there was a clear tendency for larger copepods (high PC1 group) to be more transparent (Figure 2B).

5.2 Vertical Profiles of Morphological Groups

For all groups, the 20m-binned profiles show a notable structure. While copepods were observed throughout the mesopelagic (Supplemental Figure 4), the majority of day/night differences were observed above 600m (Figure 3). For all morphological groups, there was a peak in nighttime concentration in the lower epipelagic (50m-200m). Similarly, there was a decrease in average daytime concentration over the same region. This pattern is particularly apparent for the groups which are mid and high on both PCs (Figure 3B, C, E, F). Across all groups, both average daytime and nighttime concentration were low in the upper mesopelagic (200m-300m). Then, there was a peak in average daytime concentration in the depth bins in the mid-mesopelagic (400m-600m).

5.3 Weighted mean depth analysis

The bin-constrained bootstrap approach provided a direct method to compare DVM between groups. Size (PC1) had a clear effect on DVM magnitude. First, for all PC1 groups, daytime

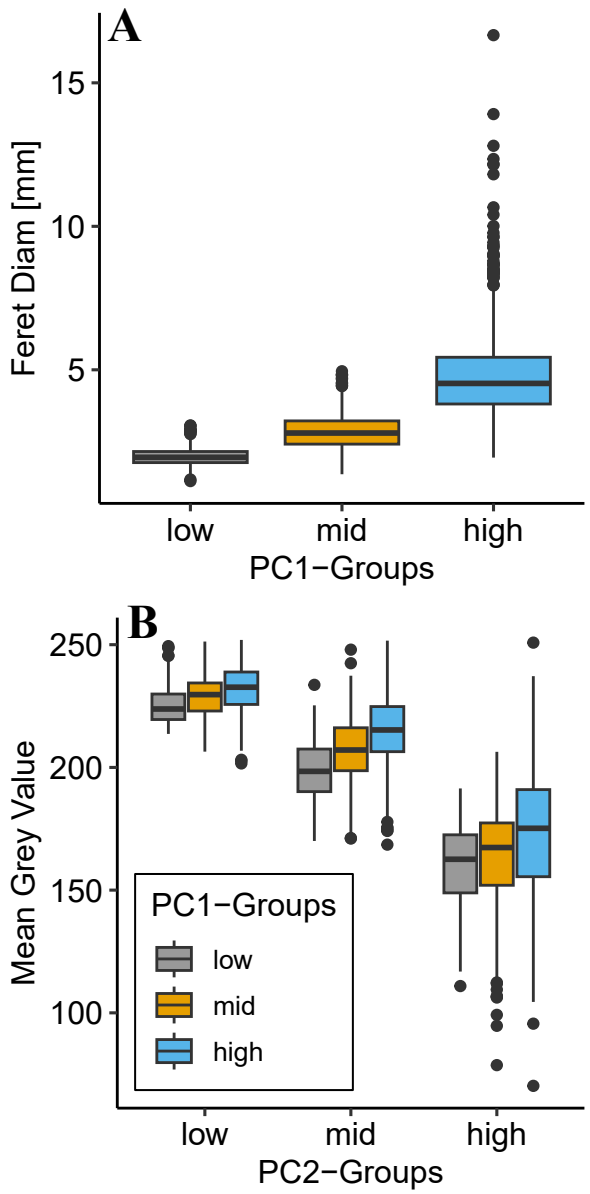

Figure 2: Comparison of morphological groups to relevant parameters. Groups were constructed along principal components with low as below 25th percentile, mid as 25th-50th percentile, and high as above 75th percentile. (A) PC1 groups are significantly different along feret diameter and display a clear trend for size. (B) PC2 groups are significantly different in terms of mean grey value. Note that a low mean grey value indicates a darker copepod.

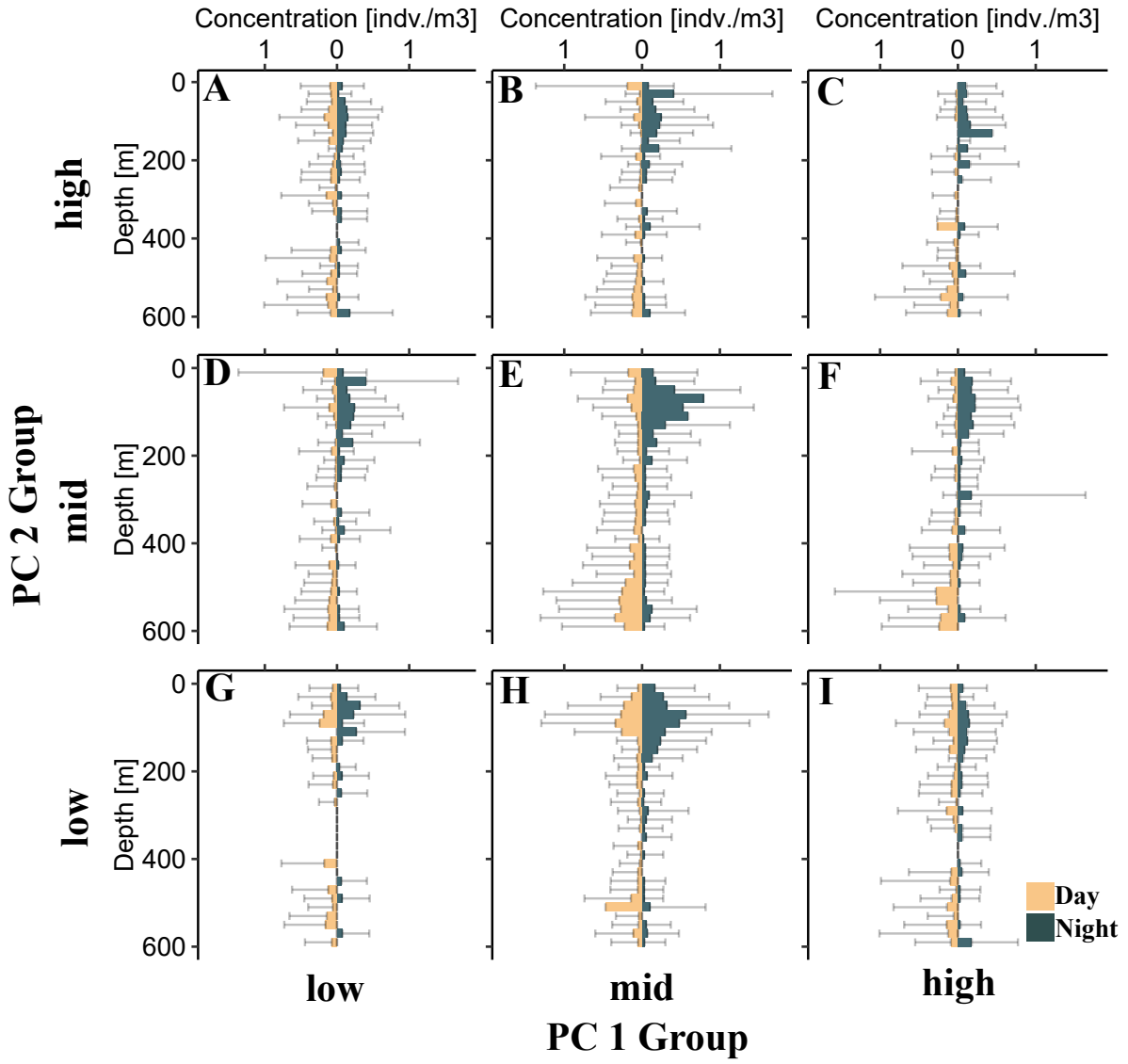

Figure 3: Average vertical profile of different copepod morphological groups. Bars display average concentration in a 20m depth bin. On each panel, left-side bars correspond to daytime while right-side bars correspond to nighttime. Standard deviation is shown for each 20m depth bin. Each panel corresponds to a morphological group along PC1 (size axis) and PC2 (transparency axis). (A) low PC1, high PC2; (B) mid PC1, high PC2; (C) high PC1, high PC2; (D) low PC1, mid PC2; (E) mid PC1, mid PC2; (F) high PC1, mid PC2; (G) low PC1, low PC2; (H) mid PC1, low PC2; (I) high PC1, low PC2

WMD 95% bootstrapped confidence intervals (95% CIs) were deeper and non-overlapping with the nighttime 95% CIs (Figure 4). This indicates a clear DVM pattern. However, the differences in day and night CIs varied between morphological groups. All PC1 groups had a similar, overlapping nighttime 95% CI in the lower epipelagic (~145m - ~200m). However, there was a clear difference in the depth of the daytime 95% CIs. The small (low PC1) group had the shallowest 95% CI (235.2m-296.0m). The mid PC1 group's daytime 95% CI was slightly deeper (309.0m-347.3m). The large (high PC1) group daytime 95% CI was even lower (352.3m-405.0m).

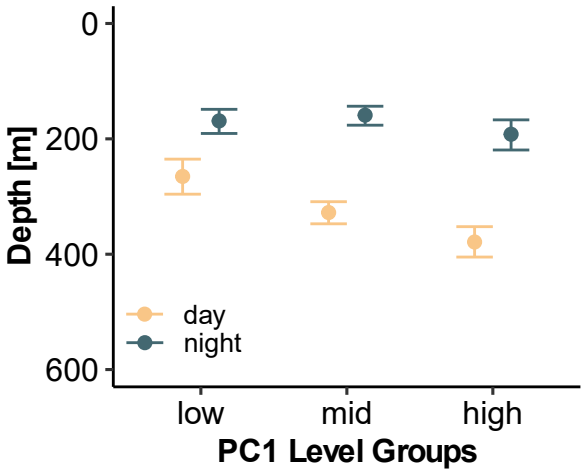

Figure 4: Mean bootstrapped weightd mean depth and 95% confidence intervals for copepods of different morphological groups. Low, mid, and high groups correspond to the different percentiles along PC1 from the morphospace. PC1 largely is explained by size metrics, with higher scores indicating a larger copepod.

When considering the influence of transparency (PC2) on DVM magnitude, we compared PC2 groups within their PC1 grouping. This approach was warranted because of the tendency for size to have a slight effect on transparency (Figure 2). At this level of comparison, there were several notable trends. For the smaller copepods (low PC1), once the data were split

into PC2 groups, the wider 95% CIs indicate little to no DVM signal. Generally, the daytime 95% CIs and nighttime 95% CIs are overlapping or near-overlapping (Figure 5A). With mid sized copepods, there was a clear DVM signal. However, all PC2 groups appeared to have a similar DVM magnitude with each group's daytime 95% CIs overlapping with each other (Figure 5B). There was a difference in DVM magnitude across PC2 groups within the largest copepods. The more transparent copepods (low PC2 group) showed no DVM signal, with a shallow daytime WMD. However, the darker copepods (mid and high PC2 groups) had deeper daytime WMDs (Figure 5c).

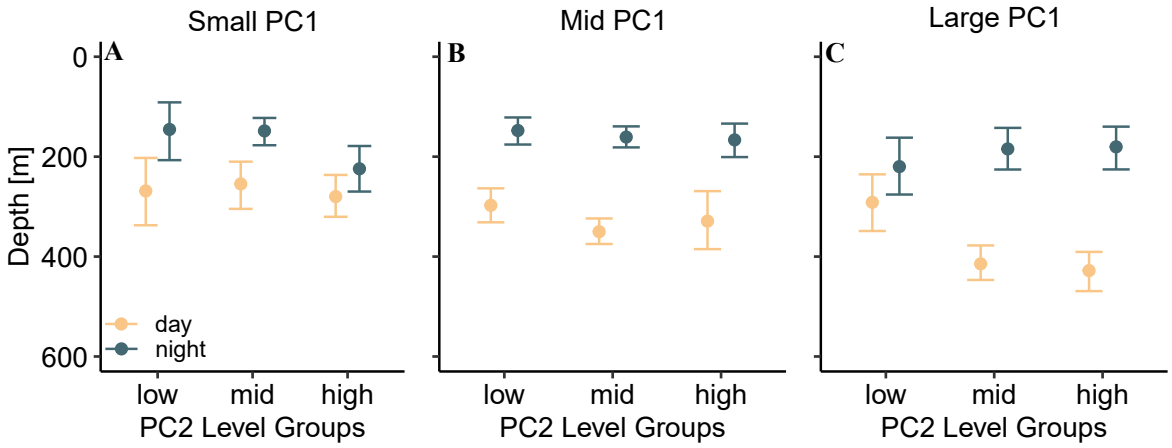

Figure 5: Mean bootstrapped weighted mean depth and 95% confidence intervals shown by copepod morphological groups along PC2 (transparency). Each panel represents a different size group of copepods (PC1 groups).

6 Discussion

6.1 Copepod morphospace

In this study, we built on methods for describing morphospaces from similar in-situ imaging studies (Vilgrain et al. 2021; Trudnowska et al. 2021; Sonnet et al. 2022). The PCA-defined morphospace with the present data aligns well with the prior applications. Interestingly, the morphospace defined on Arctic copepods by Vilgrain et al. (2021) is extremely similar to the morphospace in this study. The proportion of morphological variation explained by each of the four principle components are extremely close between these two studies. It is possible that this is an artifact of the similarity of input data. Given the UVP has a limited range of observable size classes (Picheral et al. 2010), only copepods above a certain size were fed into both PCAs. Nonetheless, it is striking that the two morphospaces are similar considering the vastly different community compositions between the Arctic ocean and subtropical gyres (Soviadan et al. 2022).

6.2 Morphology and DVM

The pattern of DVM described in this study is consistent with the general DVM pattern (Bianchi and Mislan 2016; Bandara et al. 2021). The average vertical profiles display a clear day/night difference (Figure 3). In each 20m depth bin, there was large variation, often exceeding the average concentration. This large variation however, was expected. There can be considerable variation between UVP estimates of zooplankton abundance (Barth and

Stone 2022). Additionally, in this study we pooled casts across multiple seasons. Variability in copepod DVM has been described across seasons (Whitmore and Ohman 2021). While seasonal variability in DVM is in an interesting question in the Sargasso Sea, the nature of our dataset did not lend itself to this investigation. However, despite the need to pool UVP casts across, the signal of DVM was still observable. Previous studies using in-situ imaging have also noted a signal of DVM with copepods (Pan et al. 2018; Whitmore and Ohman 2021). Yet due to small and uneven sampling, it can be a challenge to quantify DVM using in-situ imaging. As presented in this paper, bin-constrained bootstrapping offers a robust method to quantify WMD and investigate DVM hypotheses.

Copepod size had a clear effect in which larger copepods migrated further. This finding is consistent with several studies which have documented a size-dependent relationship for copepod DVM (Ohman and Romagnan 2016; Aarflot et al. 2019; Pinti et al. 2019). Ohman and Romagnan (2016) noted that moderate-size copepods had the largest migrations. While this may seem contradictory to the present study, the difference between study systems needs be taken into account. The copepods described in the large (high PC1) group had a mean feret diameter of nearly 5mm. Conversely, in Ohman and Romagnan (2016)'s study the "moderate" copepods ranged from 4mm-6mm. An effect of transparency on copepod DVM was only observed in the large copepod group. The large but more transparent copepods (low PC2, high PC1) did not have a detectable DVM signal. Yet the darker copepods (mid and high PC2) had a large DVM signal. Hays (2003) described that copepod pigmentation could explain increased DVM with small (<1mm) copepods. The lack of a transparency effect for the mid- and low

PC1 groups in our study is surprising. One possibility is that the small, transparent copepods were not well sampled by the UVP (Figure 2). Alternatively, some copepods which do not migrate may have pigmentation to avoid damage from UV radiation. While well documented, predator avoidance may not always be the primary selective pressure on copepod traits. For example, if the costs of migration are too large for some copepods, they will remain near the surface. However, these copepods then are exposed to UV light and may increase pigmentation to reduce damage. Likely the relationship between color and DVM is the result of a delicate balance of minimizing multiple ecological and biological risks (Hansson 2004; Hylander et al. 2014). Nonetheless, our results provide some support for the relationship between copepod color and DVM magnitude. Grey-value in UVP-imaged copepods can be indicative of many features beyond simply pigmentation, notably egg-sacs and gut contents (Vilgrain et al. 2021). Such characteristics vary much more between individuals and can have varied influences on DVM (PEARRE Jr. 2003).

References

Aarflot, J. M., D. L. Aksnes, A. F. Opdal, H. R. Skjoldal, and Ø. Fiksen. 2019. Caught in broad daylight: Topographic constraints of zooplankton depth distributions. Limnology and Oceanography **64**: 849–859. doi:10.1002/lno.11079

Aksnes, D. L., and A. C. W. Utne. 1997. A revised model of visual range in fish. Sarsia **82**: 137–147. doi:10.1080/00364827.1997.10413647

Archibald, K. M., D. A. Siegel, and S. C. Doney. 2019. Modeling the Impact of Zooplank-

ton Diel Vertical Migration on the Carbon Export Flux of the Biological Pump. Global Biogeochemical Cycles **33**: 181–199. doi:10.1029/2018GB005983

Bandara, K., Ø. Varpe, L. Wijewardene, V. Tverberg, and K. Eiane. 2021. Two hundred years of zooplankton vertical migration research. Biological Reviews **96**: 1547–1589. doi:10.1111/brv.12715

Barth, A., and J. Stone. 2022. Comparison of an in situ imaging device and net-based method to study mesozooplankton communities in an oligotrophic system. Frontiers in Marine Science **9**.

Bianchi, D., and K. a. S. Mislan. 2016. Global patterns of diel vertical migration times and velocities from acoustic data. Limnology and Oceanography **61**: 353–364. doi:10.1002/lno.10219

Brierley, A. S. 2014. Diel vertical migration. Current Biology **24**: R1074–R1076. doi:10.1016/j.cub.2014.08.054

Gorsky, G., M. D. Ohman, M. Picheral, and others. 2010. Digital zooplankton image analysis using the ZooScan integrated system. Journal of Plankton Research **32**: 285–303. doi:10.1093/plankt/fbp124

Hansson, L.-A. 2004. Plasticity in Pigmentation Induced by Conflicting Threats from Predation and Uv Radiation. Ecology **85**: 1005–1016. doi:10.1890/02-0525

Hays, G. C. 2003. A review of the adaptive significance and ecosystem consequences of zooplankton diel vertical migrations. Springer Netherlands. 163–170.

Hays, G. C., C. A. Proctor, A. W. G. John, and A. J. Warner. 1994. Interspecific differences in the diel vertical migration of marine copepods: The implications of size, color, and mor-

phology. Limnology and Oceanography **39**: 1621–1629. doi:10.4319/lo.1994.39.7.1621

Hylander, S., J. C. Grenvald, and T. Kiørboe. 2014. Fitness costs and benefits of ultraviolet radiation exposure in marine pelagic copepods. Functional Ecology **28**: 149–158. doi:10.1111/1365-2435.12159

Kelly, T. B., P. C. Davison, R. Goericke, M. R. Landry, M. D. Ohman, and M. R. Stukel. 2019. The importance of mesozooplankton diel vertical migration for sustaining a mesopelagic food web. Frontiers in Marine Science **6**.

Maas, A. E., L. Blanco-Bercial, A. Lo, A. M. Tarrant, and E. Timmins-Schiffman. 2018. Variations in copepod proteome and respiration rate in association with diel vertical migration and circadian cycle. The Biological Bulletin **235**: 30–42. doi:10.1086/699219

Ohman, M. D. 2019. A sea of tentacles: optically discernible traits resolved from planktonic organisms in situ H. Browman [ed.]. ICES Journal of Marine Science **76**: 1959–1972. doi:10.1093/icesjms/fsz184

Ohman, M. D., and J.-B. Romagnan. 2016. Nonlinear effects of body size and optical attenuation on Diel Vertical Migration by zooplankton. Limnology and Oceanography **61**: 765–770. doi:10.1002/lno.10251

Ohman, M. D., J. A. Runge, E. G. Durbin, D. B. Field, and B. Niehoff. 2002. On birth and death in the sea. Hydrobiologia **480**: 55–68. doi:10.1023/A:1021228900786

Pan, J., F. Cheng, and F. Yu. 2018. The diel vertical migration of zooplankton in the hypoxia area observed by video plankton recorder. IJMS Vol.47(07) [July 2018].

PEARRE Jr., S. 2003. Eat and run? The hunger/satiation hypothesis in vertical migration: history, evidence and consequences. Biological Reviews **78**: 1–79.

doi:10.1017/S146479310200595X

Picheral, M., S. Colin, and J.-O. Irisson. EcoTaxa, a tool for the taxonomic classification of images.

Picheral, M., L. Guidi, L. Stemmann, D. M. Karl, G. Iddaoud, and G. Gorsky. 2010. The Underwater Vision Profiler 5: An advanced instrument for high spatial resolution studies of particle size spectra and zooplankton. Limnology and Oceanography: Methods **8**: 462–473. doi:10.4319/lom.2010.8.462

Pinti, J., T. Kiørboe, U. H. Thygesen, and A. W. Visser. 2019. Trophic interactions drive the emergence of diel vertical migration patterns: A game-theoretic model of copepod communities. Proceedings of the Royal Society B: Biological Sciences **286**: 20191645. doi:10.1098/rspb.2019.1645

Schnetzer, A., and D. K. Steinberg. 2002. Active transport of particulate organic carbon and nitrogen by vertically migrating zooplankton in the Sargasso Sea. Marine Ecology Progress Series **234**: 71–84. doi:10.3354/meps234071

Siegel, D. A., T. DeVries, I. Cetinić, and K. M. Bisson. 2023. Quantifying the ocean's biological pump and its carbon cycle impacts on global scales. Annual Review of Marine Science **15**: null. doi:10.1146/annurev-marine-040722-115226

Sonnet, V., L. Guidi, C. B. Mouw, G. Puggioni, and S.-D. Ayata. 2022. Length, width, shape regularity, and chain structure: time series analysis of phytoplankton morphology from imagery. Limnology and Oceanography **67**: 1850–1864. doi:10.1002/lno.12171

Soviadan, Y. D., F. Benedetti, M. C. Brandão, and others. 2022. Patterns of mesozooplankton community composition and vertical fluxes in the global ocean. Progress in Oceanography

200: 102717. doi:10.1016/j.pocean.2021.102717

Steinberg, D. K., C. A. Carlson, N. R. Bates, S. A. Goldthwait, L. P. Madin, and A. F. Michaels. 2000. Zooplankton vertical migration and the active transport of dissolved organic and inorganic carbon in the Sargasso Sea. Deep Sea Research Part I: Oceanographic Research Papers **47**: 137–158. doi:10.1016/S0967-0637(99)00052-7

Steinberg, D. K., C. A. Carlson, N. R. Bates, R. J. Johnson, A. F. Michaels, and A. H. Knap. 2001. Overview of the US JGOFS Bermuda Atlantic Time-series Study (BATS): a decade-scale look at ocean biology and biogeochemistry. Deep Sea Research Part II: Topical Studies in Oceanography **48**: 1405–1447. doi:10.1016/S0967-0645(00)00148-X

Steinberg, D. K., and M. R. Landry. 2017. Zooplankton and the ocean carbon cycle. Annual Review of Marine Science **9**: 413–444. doi:10.1146/annurev-marine-010814-015924

Trudnowska, E., L. Lacour, M. Ardyna, A. Rogge, J. O. Irisson, A. M. Waite, M. Babin, and L. Stemmann. 2021. Marine snow morphology illuminates the evolution of phytoplankton blooms and determines their subsequent vertical export. Nature Communications **12**: 2816. doi:10.1038/s41467-021-22994-4

Turner, J. 2004. The importance of small planktonic copepods and their roles in pelagic marine food webs,.

Vilgrain, L., F. Maps, M. Picheral, M. Babin, C. Aubry, J.-O. Irisson, and S.-D. Ayata. 2021. Trait-based approach using in situ copepod images reveals contrasting ecological patterns across an Arctic ice melt zone. Limnology and Oceanography **66**: 1155–1167. doi:10.1002/lno.11672

Whitmore, B. M., and M. D. Ohman. 2021. Zooglider-measured association of zooplank-

ton with the fine-scale vertical prey field. Limnology and Oceanography **66**: 3811–3827. doi:10.1002/lno.11920